# Optical diagnostics of tissue pathologies based on elastic scattering properties

Diploma paper
by
Åsa Persson

Lund Reports on Atomic Physics, LRAP-169
Lund, July 1996

# Abstract

A non-invasive optical diagnostic tool for identifying malignancies in situ and in real time has been tested. The method is based on elastic scattering properties, of the microscopic structure of the tissue, over a wide range of wavelength.
The system uses a Xenon lamp, as the light source and two optical fibres. One of them transmit the light from the Xenon lamp to the tissue and the other fibre collects the diffusely reflected light. Two system has been tested. The Monochromator-system uses a monochromator and a photomultiplicator and measures one wavelength at the time. The OMA-system uses a spectrometer and a CCD-camera and measures all wavelength at the same time.
Comparisons between diffusely reflectance measurements made by optical fibres, M, and optical sphere, R has been done. The connection between them is shown to be $M=R*f^{*}$. $f^{*}$ is a function of tissue optical properties and the geometry of the device.
Experiments have been performed *in vivo* and *in vitro* on several different types of tissue. A piece of porkchop were used in optimising purpose. Following measurements were made *in vivo* on different skintypes on the human body. At last measurements were performed *in vitro* on human tissues, both normal and tumourus. The differences are shown in the area of 430-530 nm.

# Table of contents

# 1. Introduction

A central issue in many medical and biomedical applications of lasers and other light sources is the study of light propagation in tissue. For diagnostic purposes, such as non-invasive optical spectroscopy of tissues, the light that is diffusely reflected from or transmitted through the tissue may be measured. The measured reemitted light could show metabolic, physiologic or possibly the structural status of the tissue[1].
The purpose of this diploma paper was to investigate and verify an optical diagnostic tool, which measured the diffusely reflected light from different tissues for identifying malignancies in situ and in real time. An optical biopsy system, called OBS has been developed by Irving J. Bigio *et al.* at Los Alamos National Laboratory[2]. That system gave the inspiration to this diploma paper.

The method used to differentiate tissue types in that system is based on the elastic scattering properties depending of the microscopic structure of the tissue, over a wide range of wavelength. Many tissue pathologies show significant architectural changes at cellular level that will have effects on the elastic scattering properties separate from any inelastic scattering due to fluorescence. This will cause changes in the optical signature that derives from the wavelength-dependence of the registered scattering.

To make a successful treatment of cancer, one has to make an early diagnosis. First the physician observe a lesion by visual assessment. If there are some visible gross changes or if the physician suspects that there should be some, the analysis is partly accomplished *in vitro* by taking biopsies. The pathologist performs a microscopic assessment of the cell structure as cell architecture, sizes and shapes of the cell, the ratio of nuclear to cellular volume, etc. The results are then related to the *in vivo* condition of the patient. The physician is limited in the number of biopsies he/she can take and in many cases it's only likely to choose sites with visible gross changes. If there are no visible changes the physician needs a system that can make rapid measurements on a large number of sites.

The OBS collects and displays data within a minute. The tip of the optical fibre probe is in close contact with the tissue and the OBS displays the signature immediately. In this manner more sites could be assessed than with conventional biopsy technique. This method also prevents bleedings, minimises the risk of infections and prevents other complications, which follows with the conventional method.
Kimizo Ono *et al.* has developed a small size, portable fibre optic reflectance spectrophotometry system to improve the availability of non-invasive reflectance spectrophotometry in the clinical field. Different types of fibre optic probes were developed to accommodate a variety of clinical uses[3]. This portable system uses the same background theory as the OBS. Irving J. Bigio has also developed a portable OBS that is used in clinical tests[4].

Other approaches of optical biopsy are also performed. Laser-induced fluorescence spectroscopy (LIF) is one of them[5]. The tissue characterisation is here based on the collected fluorescence. LIF has its limitation when applied to complex and

heterogeneous malignant tissue, since patient to patient variations can mask the difference between similar tissues. The limitations can be eliminated by adding fluorescent dyes or drugs as targeting fluorophores. Another method is Raman spectroscopy.

The OBS uses less expensive equipment than the other techniques and a white light source instead of a laser. Data acquisition, storage and display time are less than one minute. In addition to the reduced invasiveness compared with current state-of-the art methods, does OBS offer a low-cost tissue diagnostic with a variety of potential applications.

# 2. Light in matter

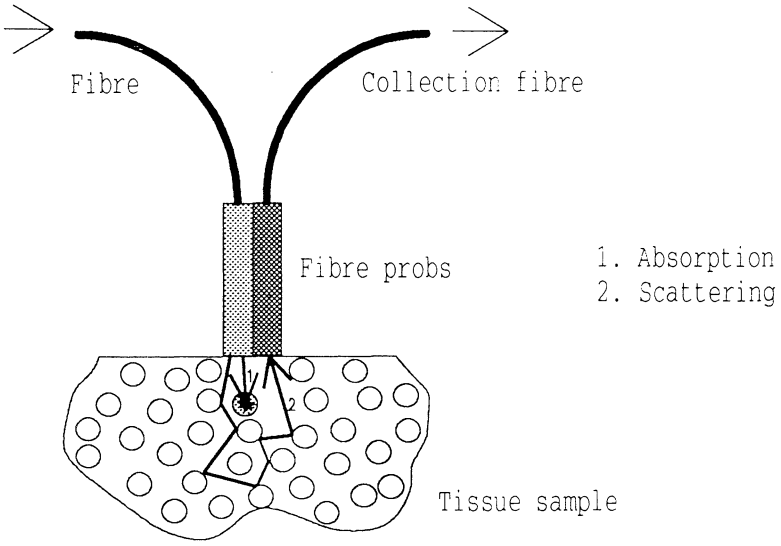


*Fig 1. The propagation of a photon in tissue. It can be absorbed or scattered.*

When photons propagate in a medium, they can undergo different types of interaction: absorption, elastic and inelastic scattering.

Matter is composed of atoms containing electrical charges, electrons and protons. An atom can interact with incoming light in two ways, depending on the incident frequency or equivalently on the incoming photon energy. If the energy of the photon match the energy of an allowed transition from the initial state, the atom might absorb the photon and a transition to the matching excited level will take place - absorption. After a short time the atom will return to the initial state and at the same time release resonance radiation. The time elapsed before the atom decays is called lifetime.
It is also possible that an excited atom will return to energy levels higher than the initial level. The emitted photon has a lower energy than the incident photon. This process is called fluorescence. The atom could also return to a lower-lying level in a system of another multiplicity, through inter system crossing. The atom may stay there for a long time, since the transition to the ground state is normally forbidden. A weak light will be emitted for some time, after the excitation has taken place. This process is called phosphorescence[5].

In contrast to the absorption process, scattering occurs if the incoming photon energy does not match excited state energies. The scattering process can be elastic or inelastic. The electromagnetic field of light makes the electron cloud oscillate with the same frequency as the incident light and the system will immediately begin to radiate at the same frequency. The resulting scattered light consists of photons with the same energy as the incident photons. This kind of scattering is elastic. If the wavelength of light is equal or larger than molecular diameter the process is called Rayleigh scattering and the probability process is proportional to $\lambda^{-4}$. In contrary if the wavelength is less than the size of the scattering particle, the process is called Mie-scattering. This process is proportional to $\lambda^{-2}$. If an external oscillating field is applied

there can be a coupling between the applied internal oscillations and the molecular vibrations. This phenomenon is called the Raman effect and represents inelastic scattering. The Raman scattering always appears together with Rayleigh scattering. Fluorescence that was described earlier is also an inelastic process.
Most of the light that is absorbed by molecules is not re-emitted. The energy is distributed among the molecules, their motions are increased and thus the temperature increases[5].

## 2.1 Tissue

Tissue is composed of cells functioning together to carry out specialised activities. The structure and properties of a specific tissue are influenced by several things. The connections between the cells, the nature of the extra cellular material that surrounds the cells and the function of the tissue.

When cells in some area of the body start to divide without control, the excess of tissue that develops is called a tumour. Tumour may be malignant and sometimes fatal, or they may be quite harmless. Malignant tumour is a cancerous growth invading the host tissue. Cells of malignant tumour duplicate continuously, without control and often very quickly. These cells can also be spread to other parts of the body, yielding metastases. A benign tumour is a non cancerous growth not invading the host tissue and this is not spread to other parts of the body[6].

### 2.1.1 Optical properties of tissues

The optical properties of tissue are important for diagnostic purpose. The absorption of tissue depends on the different constituents of tissue. Haemoglobin in blood, water and melanin are important tissue absorbers. These substances thus contribute to the shape of for instance a tissue absorption plot versus wavelength. The other tissue optical property, the scattering falls relatively smooth it falls with increasing wavelength approximately as $d^{-3}$.
There are several techniques to measure the tissue scattering and absorption coefficients separately. Most of them are useful in the region 650-1300 nm (the optical window), where the tissue absorption is low and the dominant attenuation is scattering. In this diploma work diffuse scattering in the wavelength range of 400 - 700 nm has been investigated.

## 2.2 Transport theory

Transport theory describes in theory the way light travels in tissue. The propagation of the photon is here described with the same mathematics as the transports of heat or particles in a medium and the wave-like properties of light are assumed less important for how the light propagate. The optical properties used to describe light interacting with tissue in transport theory is the scattering and absorption coefficients, $\mu_s$ and $\mu_a$

and the scattering phase function, g being the probability function for the angular distribution for a single scattering event.
The coefficients, $\mu_S$ and $\mu_a$, describe the probability of scattering and absorption of a photon per unit pathlength. Most of the phase function can be reduced to the so called g-factor defined as the mean value of the cosine of the scattering angle. These coefficients can be obtained by different kinds of measurements in combination with numerical calculations or simulations.

When light passes through a material the direct beam looses its intensity according to Beer-Lambert law[5]:

$$I(x)= I_0 \exp(-(\mu_a+\mu_S)\, x) \qquad (1)$$

The directly transmitted intensity at a distance x will be I(x) if light of original intensity $I_0$ travels in a material with a total interaction coefficient $\mu_t'=\mu_a+\mu_S$.

The radiance $L(\bar{r},\bar{s})$ ($W*m^{-2}*sr^{-1}$) is the amount of light passing position x per unit time interval in the direction of the unitvector $\bar{s}$. On one hand this light is attenuated by absorption and scattering reducing the radiance but, at the same time will light that is scattered from $\bar{s}'$ direction into the direction of $\bar{s}$ in $\bar{r}$ add as a source for the radiance and increase it. These light interactions can thus be described more formalistically by the radiative transport equation:

$$\bar{s}\cdot\nabla L(\bar{r},\bar{s}) = -(\mu_a+\mu_s)L(\bar{r},\bar{s}) + \mu_s\int_{4\pi} p(\bar{s},\bar{s}')L(\bar{r},\bar{s}')dw' \qquad (2)$$

dw' is the differential solid angle in the direction $\bar{s}'$ and $p(\bar{s},\bar{s}')$ is the phase function[7]. A distribution that is often used in tissue optics is the Henyey-Greenstein phase function[8]:

$$p(\bar{s},\bar{s}') = p(\cos\theta) = \frac{1}{4\pi}\frac{1-g^2}{(1+g^2-2g\cos\theta)^{3/2}} \qquad (3)$$

Where $\theta$ is the deflection angle. The value of g can vary between -1 and +1. If g=-1 the light is completely backscattered and if g=+1 the light is completely forward scattered g=0 means isotropic scattering. When light is scattered by particles larger than the wavelength of the light, the scattering is forward directed. This is the case for tissue.

The most common approximation of the transport equation is the diffusion theory resulting in possibilities to an analytical solutions for simple geometry's. This theory is assuming diffuse photon fluence. This can be valid if the light is multiple scattered many times. This is the case if

$$\mu_a << \mu_S\,(1-g) \qquad (4)$$

one study light that has travelled some distance within the tissue. This assumption is frequently used to calculate the light fluence in homogeneous infinite tissues. In this geometry the diffusion equation can be solved both in time and frequency domains. There are three levels of complexity of the geometry in solving the diffusion equation in time domain:

1. an absolute infinite homogeneous matter
2. a semi-infinite homogeneous medium, a slab
3. an inhomogeneous medium and other geometry's

The two first levels can be solved analytically while the last case must be solved numerically or with simulation techniques. In that case, point-like variations of scattering and absorption coefficients are often introduced as homogeneities. The variations of the optical properties can also be introduced as perturbations. In backscattering mode, when light is detected on the same side of tissue as it enters, the light distribution will follow a bent path between the source and the detector, often referred to as a banana-path[8].

For the more difficult sample geometry's, no analytical solution to the light transport can be found therefore numerical methods and simulations are used to model the light propagation in tissue. Two numerical methods that are often used, inverse Adding-Doubling that take into account anisotropic scattering and Monte-Carlo simulations[9].

The Monte-Carlo technique is a simulation method often used to calculate the way light travel inside turbid media such as tissue. This technique is considered to be accurate and flexible. The photon is traced through the tissue until it exits or is terminated due to absorption. The photon tracing process is repeated a large number of times. This makes it possible to obtain statistics for a physical parameter, like the absorption position, the exiting position etc. The simulations are made in two steps:

1. The step size between each interaction site is randomised as $-\ln(\xi) / (\mu_a+\mu_s)$
   ($\xi$ is a random number between 0 and 1)
2. The photon weight is decreased by a factor of $\mu_a/(\mu_a+\mu_s)$

When the random walk is finished one can obtain the light fluence[10].

## 2.3 Mathematics of reflectance

The reflectance, R, is defined to be the ratio of the reflected power and the incident power.

$$R = \frac{I_r A \cos\theta_r}{I_i A \cos\theta_i} = \frac{I_r}{I_i} \quad ;\theta_i = \theta_r \qquad (5)$$

A is the cross-sectional area. $I_r$ and $I_i$ are the reflected and incident flux densities[11]. In this paper $I_i$ is the intensity of the direct lamp light and $I_{ref}$, $I_{tissue}$ are the intensity of the diffuse reflected light from the reference material- the highly reflecting barium sulphate, and the tissue, respectively.

$$R_{ref} = \frac{I_{ref}}{I_i} \cong 0.992^{9} \quad (6)$$

$$R_{tissue} = \frac{I_{tissue}}{I_i} = \frac{I_{tissue}}{I_{ref}} \cdot 0.992 \quad (7)$$

$R_{ref}$ and $R_{tissue}$ are the diffuse reflectance of the reference and the tissue, respectively[11].

### 2.3.1 Reflectance spectroscopy with optical fibre devices

The set-up used in these measurements was an optical fibre based system
There are several components which influence measurements with an optical fibre device. The measured signals depend on the emission spectrum of the light source ($S(\lambda)$), the detector response for various wavelength ($D(\lambda)$) and on the fraction ($f(\lambda)$) of total reflectance collected by the fibre device. By forming the ratio of two measurements the $S(\lambda)$ and $D(\lambda)$ are cancelled from the result. This was utilised by evaluating the ratio of the measurement on tissue and the reference, denoting the result, M[12].

$$M = \frac{S \cdot R_{tissue} \cdot f_{tissue} \cdot D}{S \cdot R_{ref} \cdot f_{ref} \cdot D} = R_{tissue} \frac{f_{tissue}}{R_{ref} \cdot f_{ref}} = R_{tissue} \cdot f^{*} \quad (8)$$

$f^{*}$ is a function of tissue optical properties and the geometry of the device.

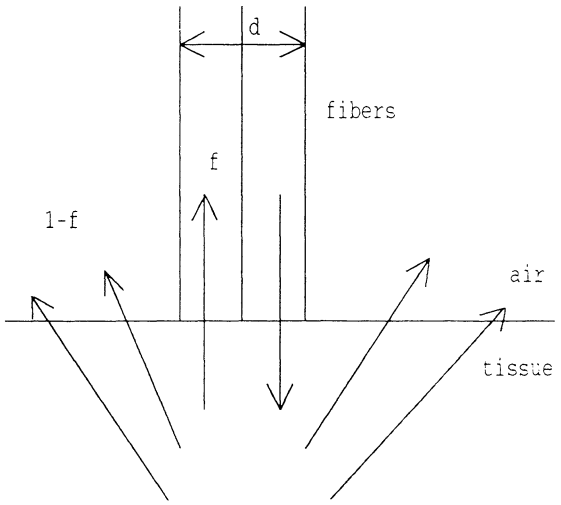


*Fig 2. Optical fibre collects a fraction f of the total diffusely reflected light.*

With the geometry used in this work, with the leading and receiving fibres next to each other the behaviour of f is documented as a function of three parameters:

1. the mean free path, mfp´ [cm]
2. the optical penetration depth, $\delta$ [cm]
3. the fibre diameter, d [cm]

The collection fraction f is described as[12]

$$f = (1 + \tanh(x)) \div 2 \tag{9}$$

$$x = A\left(\ln\left(\delta \cdot mfp' \div d^2\right) + B\right) \quad ; \text{A, B constants} \tag{10}$$

$$mfp' = \frac{1}{(\mu_a + \mu_s')} \tag{11}$$

$$\delta = \sqrt{mfp' \div 3\mu_a} \tag{12}$$

## 2.4 Interaction between light and tissue

Consider light as electromagnetic waves. When the wave passes from one medium to another with different refraction indices, one part of the wave will be reflected backwards and one part will be transmitted as a refracted wave. There are two types of reflection: Specular reflection, which occurs when the surface is smooth, and the diffuse reflection, which is obtained by the light photons who has interacted with the tissue[11].

Consider light as electromagnetic waves. When the wave passes from one medium to another with different refraction indices, one part of the wave will be reflected backwards and one part will be transmitted as a refracted wave. There are two types of reflection: Specular reflection, which occurs when the surface is smooth, and the diffuse reflection, which is obtained by the light photons who has interacted with the tissue[11].

Biological tissue is an optically turbid medium that contains structures of various sizes. Because of that, tissue is a scattering and absorbing medium and the refractive index is higher than for air (approximately 1.4). Light can be absorbed by chromophores (the name of various absorption centres in tissue). There is a large number of different chromophores in cells, for example vitamins, flavins, NADH, haemoglobin, proteins, etc. The absorption of chromophores is strongly wavelength-dependent and they may absorb in the UV, the visible and/or near-IR region. Water is also an important absorbant and it absorbs in the UV below 200 nm and in IR-region. Tissue also consists of a large number of scattering centres. They are small regions with a refractive index that differs from the surroundings, for example membranes of mitochondria's and whole cells.
When light passes the interface from air to tissue, 2-4% will be reflected and the remaining light enters the tissue and will go through scattering and absorption processes. In the ultraviolet and visible wavelength-region below 600 nm both the scattering and absorption coefficients are high. Above 600 nm the scattering coefficient generally dominates over the absorption. It is therefore in this wavelength-region expected that most of the light is scattered[13].
The light that is scattered backwards exiting the tissue at the same surface as if entered after one or several scattering processes is also called diffusely reflected light.

It is the diffusely reflected light that is collected and investigated in this diploma work. It is possible to treat the light as Rayleigh scattered or Mie scattered, depending on the size of tissue particles responsible for the scattering. In tissue both sizes contributing to Rayleigh and Mie scattering are present.
I.J.Bigio has found that the cellular components of the tissue that causes most of the elastic scattering event dimensions comparable or larger than the wavelength of visible to near-IR light[14]. This leads to believe that the dominant scattering is Mie scattering.

### 2.4.1 Elastic scattering as a diagnostic tool

As mentioned before, many tissue pathologies, such as malignancy, cause changes in the cellular and molecular structure. These changes could be expected to effect the elastic scattering properties. The wavelength-dependence of elastic scattering gives consequential changes in the optical signature. Therefore can elastic scattering spectroscopy be used as a diagnostic tool for malignancy and other tissue abnormalities. The diffusion theory or Monte Carlo methods are most commonly used among researchers to describe light transport in tissue. Diffusion theory is only valid when the source and the detector are well separated. This is not possible when small tissue volumes are to be examined. The source and the detector most then be placed close together. A combination of Mie scattering theory and Monte Carlo techniques could be used to model the scattering procedure[14]. Results from such calculations form the basis for experiments performed in this diploma project.

# 3. Material and methods

## 3.1 The Set up

Two setups have been used. One optical system, which measured one wavelength at a time and was using a monochromator as a spectral resolution instrument and a photomultiplier as a detector. The other system registered a whole spectrum at the same time. It was an optical multichannel analyzing (OMA) system using a grating spectrometer as a spectral resolution instrument and a CCD camera as a detector.

### 3.1.1 Monochromator-system

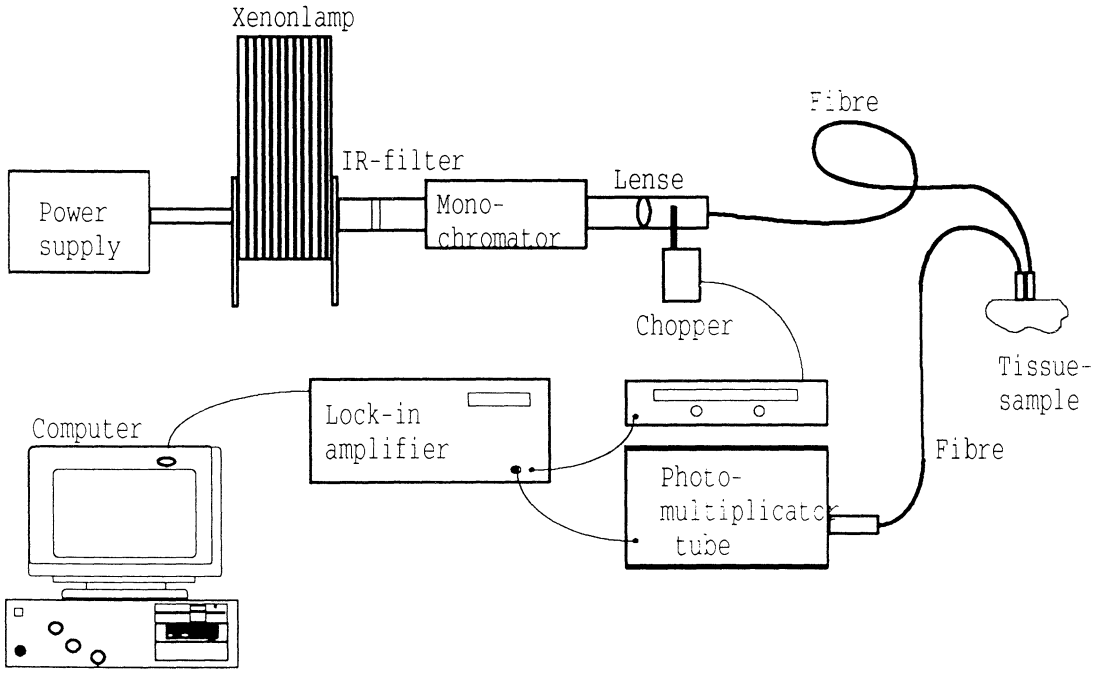


*Fig 3. The set up for the monochromator system*

The set up for the monochromator system is shown in figure 3. A 75-W high-pressure Xe lamp was used as a light source yielding a broad wavelength distribution see further figure 14 in the result chapter. The light passed through a monochromator with which the wavelength was selected. A computer controlled steping motor was connected to the monochromator . The size of steps and wavelength range could be varied and set in a program. In this study spectra from 400-800 nm were recorded with a 5 nm resolution. The resulting light beam was focused into a 400 μm fibre made of almost fluorescence free quartz. Another similar 400μm fibre guided the collected diffusely reflected light into a photo multiplier tube (PMT; Hamamatsu R928). The fibres were placed close together to receive as much light as possible. A black tape between the fibres prevented the light from entering the detector fibre without interacting with the tissue. The fibres were placed in direct contact with the

tissue surface to avoid specularly reflected light from entering the detector fibre. The signal from the photomultiplier was fed to a lock-in amplifier (Stanford Research System, model SR830). The lock-in amplifier was able to dispose the background light as the light was chopped. Finally all results were fed to the PC controlling the measurements.

### 3.1.2 OMA-system

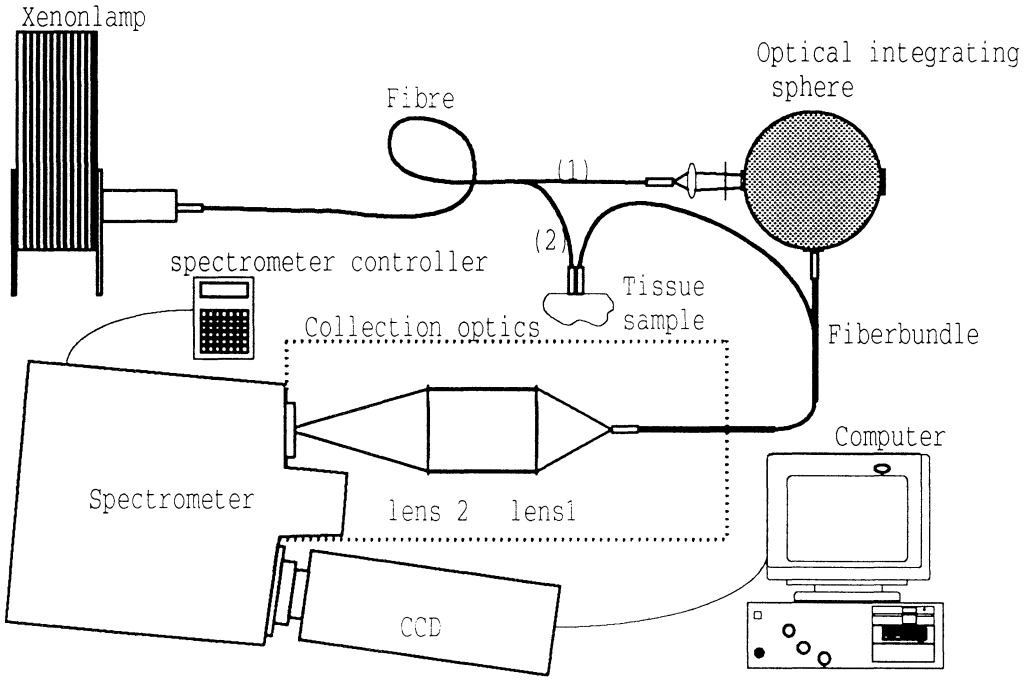


*Fig 4. The set up for the OMA-system, with both optical integrating sphere (1) and optical fibre(2) arrangement.*

Two different measurement geometries were employed, either the two-fibre probe described above, or an optical integrating sphere collecting all diffuse reflected light. The same 75-W high pressure Xe lamp described above was used as a light source. The light beam was focused into a 400 μm fiber, guiding the light directly to the tissue or to an optical integrating sphere. The diffusely reflected light was guided by a fibre or a fibrebundle used for the two measurement geometries, respectively, back to the collection optics at the spectrometer. The fibers in the fibre bundle were mounted in a circle at the entrance of the fibre bundle and in a line at the exit to fit the entrance slit of the spectrometer. The collection optics was composed of two lenses. Lens 1 was aimed to collimate the scattered light and Lens 2 was used to focus the light onto the entrance slit of the spectrometer. Either of two similar Czerny-Turner grating spectrometers were used in the recordings. Two gratings were available, a 150g/mm grating blazed at 500 nm and a 1200g/mm grating blazed at 750 nm. The width of the entrance slit of the spectrometer could be set in steps of 6.25 μm between 0 and 7000 μm. All moving parts were controlled remotely by a spectrometer controller. In this diploma work a 150g/nm grating was used and the entrance slit was adjusted to 550 μm or 400 μm, respectively. When the light beam has passed the spectrometer the light was detected by a CCD detector system. The CCD detector was an OMA-vision

CCD detector manufactured by EG & G Princeton Applied Research. The entire detector system was composed of a CCD camera (Thomson CSF THX-31159 A), an OMA-vision controller board, an OMA-vision power block, and a PC. The wavelength range of detection was either 300-900 nm or 460-700 nm depending of the spectrometer used. The CCD camera was cooled with liquid nitrogen. Since the dark current decreases with temperature, it is of great importance to keep the temperature as low as possible. The CCD camera could be cooled in the temperature range from - 80°C to - 140°C. The signals from the CCD camera were fed to the PC, where the diffusely reflected light spectrum was displayed and stored in real time.

An optical integrating sphere has been used to collect all the diffusely reflected light. At the end of the 400 μm source fiber the light beam was collimated with a 2.5 cm-focal-length lens and an aperture stop. The sphere (Oriel) was 20.3 cm in diameter, and its inner surface was covered with barium sulfate. The highly reflecting inner surface allowed light entering the sphere from any direction to be collected with the same efficiency by the fibrebundle mounted at the sphere surface. The two beam ports of the sphere were placed opposite to each other. The light beam entered the first port and the exit port was covered with a sample. The diffusely reflected light was collected with the fibre bundle and guided to the spectrometer.

## 3.2 Tissue specimen

Experiments have been performed *in vivo* and *in vitro* on several different types of tissue.

Spectra of diffusely reflected light from both animal and human tissue were recorded. Tissue from porkchop and loin of pork was used in a pre-study. The meat was simply bought in nearest grocery's, fresh or a few days old. The tissue samples were about the same size as they used to be in the shop, 1-1.5 cm thick and 15-20 cm wide. A number of spectra on fat, muscle and bone tissue have been collected in order to check if differences in the recorded reflectance spectra from the different tissue types were obtained.

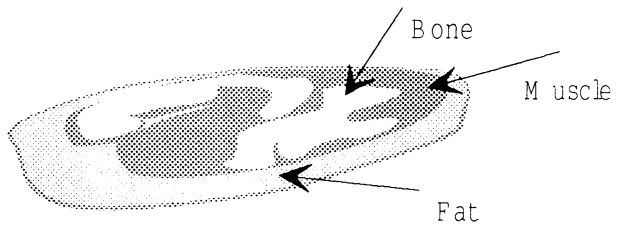


*Fig 5. A piece of porkchop, where bone, muscle and fat tissue are pointed out*

The first measurements on human tissue were made *in vivo* on different external parts of volunteers. Measurements were made outside and inside the cheek, on the earlobe, at the front tooth, etc. Spectra have also been taken on parts of the hand; on the skin on the top of the hand, inside the palm, on the knuckle, on the nailtip, on the fingertip and on the vein on the wrist. . Measurements were also performed *in vitro* on various human tissue samples. These samples were received from the department of

Pathology at Lunds University Hospital. The sizes of the samples were in the range of 0.5-1 cm thick and 1-5 cm wide. Different types of samples were investigated. One sample contained normal and metastatic liver tissue. The liver tumour was originating from an ovary tumour. There were also samples from normal and metastatic lung tissue. The metastasis originated from a kidney tumour. There were finally also samples from normal and tumour testis tissue.

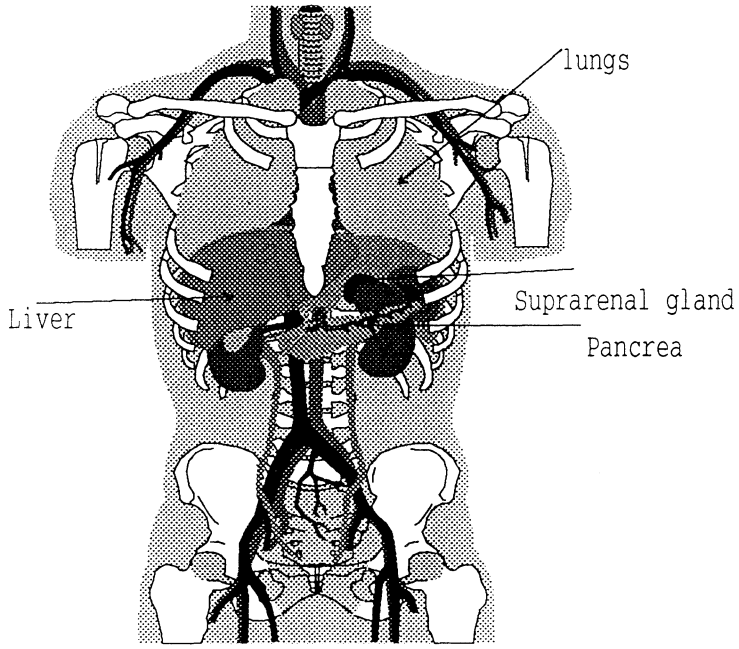


*Fig 6. A cross section of the upper part of the human body. Lungs, liver, pancreas and suprarenal gland are pointed out.*

## 3.3 Methods

### 3.3.1 Optimisation of the systems

Before any measurements with the monochromator could take place, the light path had to be carefully adjusted to obtain as good signal as possible. For this purpose spectra were collected, using a test surface covered with highly reflecting barium sulphate with a well-known reflectance (R=0.992 for all visible wavelengths). Comparison between different spectra showed that there were major fluctuations on the lamp light intensity. Several attempts were made to get rid of these fluctuations. The spectrometer systems were both well optimised and only minor adjustments were made.

### 3.3.2 Measurement procedure with optical fibre

The tissue sample was placed on a plate. The source and detector fibre were fixed as close together as possible with black tape as a probe. The two fibre probe was then fixed in a holder. The probe was in contact with the examined tissue during recording.

A spectra was collected and stored in the computer. The results were presented on the computer screen as a row data representing the intensity of the collected light as a function of wavelength, $(I*f)_{tissue}$. The sample was then replaced with the barium sulphate plug and another spectrum was collected, $(I*f)_{ref}$.
A ratio of the measured tissue spectra and the reference spectra were formed to eliminate the influence of the lamp emission spectra, detector response, fibre transmission etc.
Mean values of at least three measurements were always calculated for both tissue-sample-spectra and reference-plug-spectra before forming this ratio.
A ratio of the meanvalue-spectra was made and then plotted versus the wavelength.

$$M = \frac{(I*f)_{meanvalue,tissue}}{(I*f)_{meanvalue,ref}} \qquad (1)$$

### 3.3.3 Measurement procedure with optical sphere

In these measurements, the exit port on the sphere was covered by the tissue sample. A spectrum was collected and stored in the computer. The barium sulphate reference plug was replacing the tissue sample on the exit port and an additional spectrum was collected and stored. A ratio of both spectra was formed and plotted versus the wavelength.

## 3.4 Data evaluation

*In vivo* measurements have been used to evaluate differences between measurements using the optical fibre probe and the optical integrating sphere. Comparisons between M and R spectra of the same tissue and of different tissues were made. Plots are presented to illustrate the difference between M and R for the two measurement geometries.

The relationship between M and R is M/R = f. This is explained closer in chapter 2.3. Comparisons between f-spectra of different tissue types have been made. When the optical penetration, $\delta$, and the mean free path, mfp', increases, more light escapes outside the collection area of the fibre, and f drops. When f decrease, also $(\mu_s' + \mu_a)$ will decrease (Fig.7).

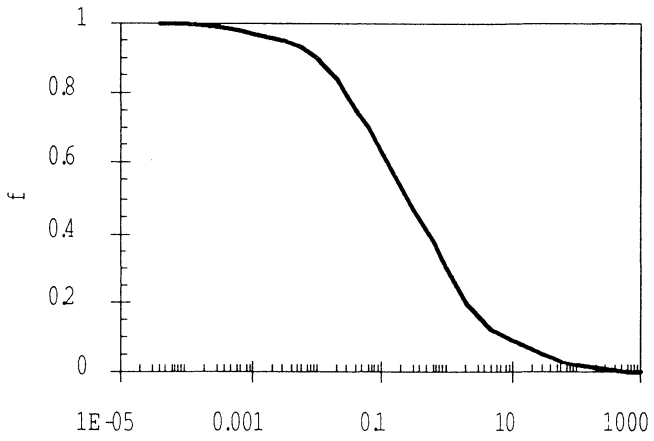


*Fig 7. Collection fraction, f, as function of optical properties and fibre diameter*[12].

An absorption spectrum for blood has be an absorption spectrum for blood (Fig 8.) has been used to relate differences in $\mu_a$ of different tissues to make some conclusions of the behaviour of $\mu_s$'. It is known that as the absorbance of a medium increase, the probability that photons survive as they encounter scattering events decreases[6]. The oxyhemoglobin spectrum is usually seen *in vivo* in skin, although the deoxy-Hb spectrum is not uncommon[12].

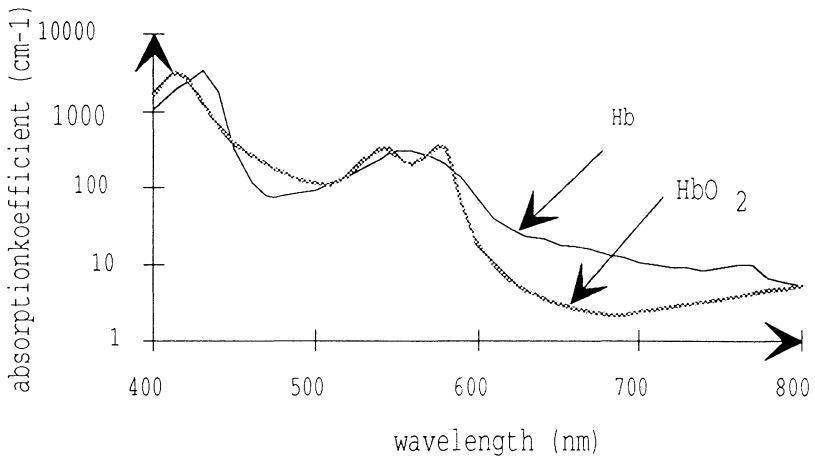


*Fig 8. Absorption spectra of Hb and* $HbO_2$[15].

The absorption spectrum has also been used when the *in vitro* spectra have been evaluated. There is a difference in blood contents between malignant and non malignant tissue. This indicates by the different behaviour of $\mu_s$' and $\mu_a$.

An analysing procedure described more complete by S.L. Jacques [12] has been used to analyse the optical fiber measurement, M. The epidermal melanin content and cutaneous blood content could be in the skin measurements determined by analysing the curves. An optical density (OD) curve was used as analysing curve with OD calculated from M as

$$OD = - \log (M) \qquad (2)$$

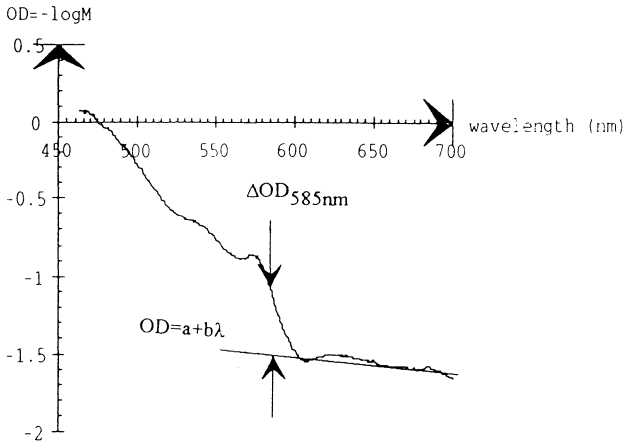


*Fig 9. A OD spectra from author's forearm.*

The OD curve was fitted by linear regression in the 650-700 nm wavelength range to yield a straight line:

$$OD = a + b\lambda \qquad (3)$$

It has been shown that the epidermal melanin content is proportional to the slope b[OD/nm] of this curve more conveniently expressed as a, pigment slope parameter b'[-OD/nm*$10^6$], so that the slope increases as melanin increases. The melanosom volume fraction $f_{mel}$ can be estimated as[12]

$$f_{mel} = (\text{pigment slope} - 600)(0.0126[\%/\text{slope}]) \qquad (4)$$

Where the numbers 600 and 0.0126 were given from calibrations in that paper. The slope for the case of zero melanin content is 600[-OD/nm*$10^6$] and a comparison factor derived from the theoretical values of $f_{mel}$ and the pigment slope was found to be 0.0126 [%/slope]. This data yields the forearm of S. L Jacques and the formula is calibrated only for the measurements presented in Ref. 12, and it is used in this paper for comparison purpose only. The cutaneous blood content could be characterised by the ΔOD spectrum at 585 nm, defined as the difference between the measured curve and the extrapolated fitted curve (see Fig 9). The equivalent uniform blood content of the skin can be estimated:

$$\%\ \text{blood content} = \Delta OD_{585}(4.5[\%/\Delta OD_{585,blood}]) \qquad (5)$$

Where the number 4.5 again is taken from Ref. 12. A comparison factor derived from the theoretical value 0.2% equivalent tissue blood, content corresponding to 0.044 ΔOD, is $4.5[\%/\Delta OD_{585,blood}]$.

# 4. Results

## 4.1 Optimising the Monochromator-system

In the beginning there were troubles with fluctuation from the lamp and the intensity of the lamp light was not adequate. Several parameters were investigated to see what influence they have on the measurements:

- equipment
- surrounding light sources
- increasing the slit width of the monochromator
- to use two fibres with outgoing light, one to measure the lamp spectrum and one to measure the tissue spectrum.
- mean values of a couple of measurements
- dwell time and time constant of the lock-in amplifier

### 4.1.1 Surrounding light sources and equipment

Measurements were made directly, 1 h, 1.5h and 2 h after turning on the Xenon lamp and the lock-in amplifier (Fig 10).There have also been made measurements with surrounding light sources on or in total darkness (Fig 11).

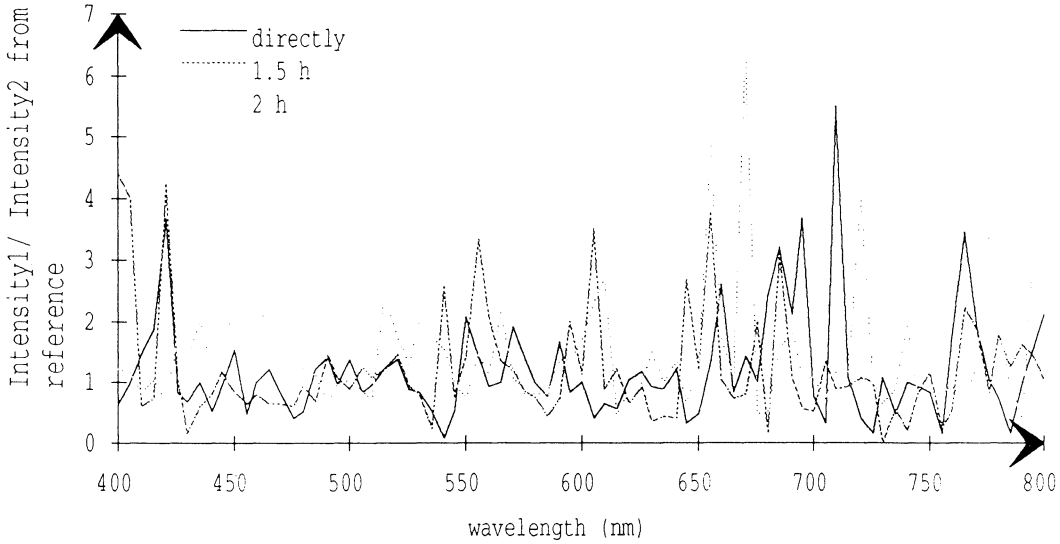


*Fig 10. Comparison between different measurement series, that are started directly, 1.5 h or 2h after the equipment was turned on.*

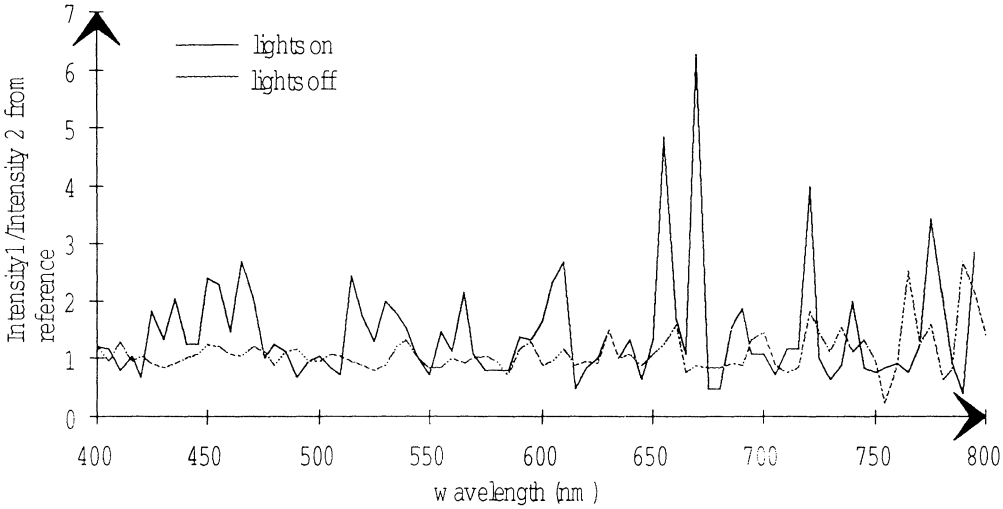


*Fig 11. Comparison between two measurement series which were recorded 2h after the equipment was turned on with room lights on or off*

The equipment should be turned on at least two hours before any measurements takes place (Fig 10). Surrounding light sources should be turned off during measurements. The influences of surrounding light sources are shown in Fig 11.

### 4.1.2 The use of more than one fibre

By measuring both the tissue and the reference spectra simultaneously using two channels, one might get rid of the fluctuations and minimises the measuring time. The difficulties would in this case be to focus the light at the fibres and to get the same amount of light into both fibres. This is necessary because when one is creating the ratio between $I_{tissue}$ and $I_{ref}$ to get the reflectance $R_{tissue}$, $I_i$ has to be the same on both fibres (see chapter 2.3.).

### 4.1.3 Mean values

Mean values of a number of measurement series were calculated by the computer. Comparisons between mean value of three and five measurement series have been made for exactly the same position of the fibres.
During this test the dwell time was 5 seconds and the time constant 3 seconds. The sample was a porkchop.

Many fluctuations disappear already when mean value of three series were used. There was no big difference between the three and five series (Fig 12) and to minimise the measurement time the mean value of three series could be exceptable.

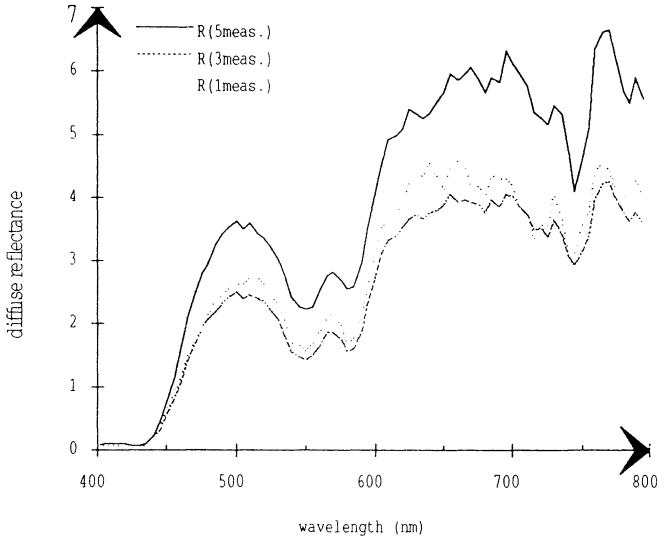


*Fig 12. Difference between 5, 3 or 1 meanvalues of measurements*

### 4.1.4 Dwell time and time constant

Different combinations of dwell time and time constant on the lock-in amplifier have been tried as well (table 1). The palm of the hand was used as a sample and the mean value of three consecutive recordings was used. They are presented in figure 13.

With the dwell time set to 5 seconds the most noise-free spectrum was obtained with as high time constant as possible, in this case 3 seconds. Comparisons between different dwell times yield better spectra with a large dwell time, here 5 seconds.

| Name of the measuring serie | Dwell time (s) | Time constant (s) |
|---|---|---|
| hand 5:3 | 5 | 3 |
| hand 5:1 | 5 | 1 |
| hand 5:0.3 | 5 | 0.3 |
| hand 3:1 | 3 | 1 |

*Table 1. Several combinations of dwell time and time constant have been made to get rid of fluctuations.*

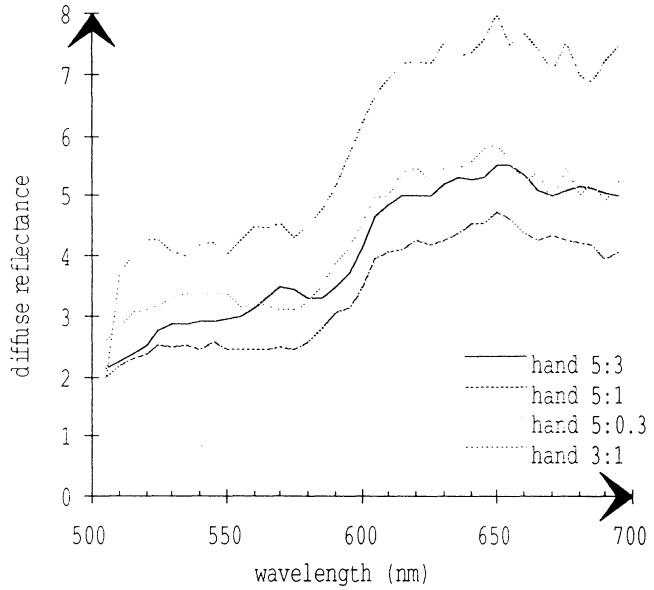


*Fig 13. Spectra of the diffuse reflectance with different combination of dwell time and time constant. The sample in these recordings was the palm of the hand.*

## 4.2 Monochromator-system

Measurements were made on the referens sample and on a porkchop (figure 14 and figure 15). These spectra were used during the optimising procedure and to compare results with those obtained with the OMA- system.

Measurements on the porkchop were made both on muscle and fat tissue. The spectras show differences in the area of 430-600 nm (figure 15).

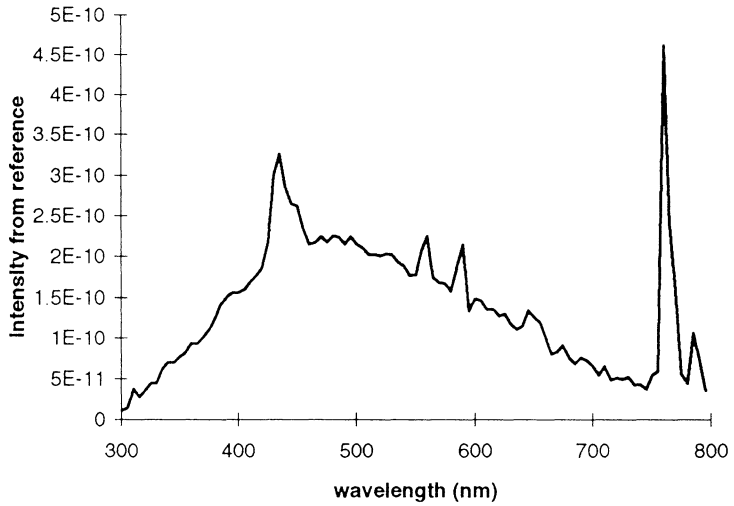


*Fig 14. The intensity of the diffuse reflected light from the reference sample( mean value of three recordings).*

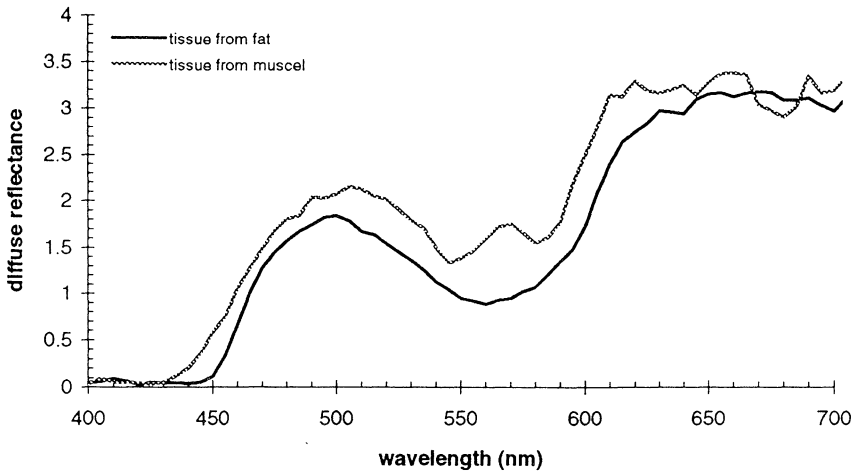


*Fig 15. The diffuse reflectance from muscle and fat tissue on a porkchop .*

At this stage, when the system was optimised, spectra from various tissues were collected. The first measurements were recording from the palm of the hand and from the light skin on the forearm (fig 16).

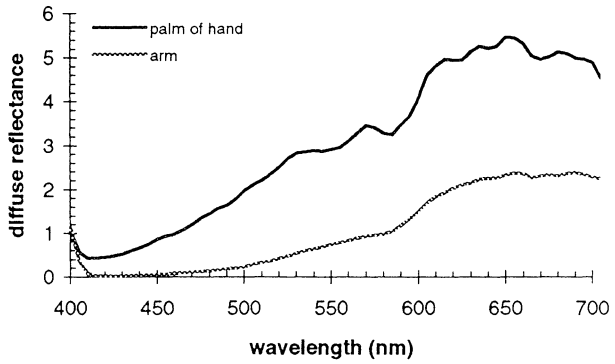


*Fig 16. Diffuse reflectance from the palm of the hand and from the light skin on the forearm*

Several measurements were also recorded from an *in vitro* sample of pancreas and a tumour from the same pancreas.

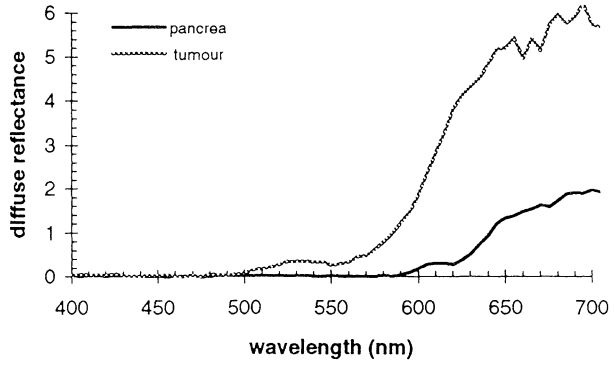


*Fig 17. Diffuse reflectance from non-malignant and malignant pancreas.*

The tumour reflects more light than the normal tissue and the difference between the spectra are mainly found in the area of 500-590 nm.

## 4.3 OMA-system

Firstly, measurements on the reference sample were made and then some measurements on a chop of pork were made to be used for comparisons with the Monochromator-system (figures 18 and 19).

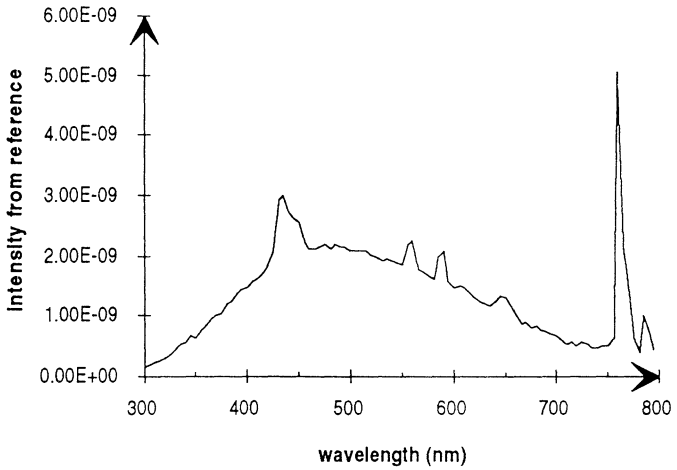


*Fig 18. Intensity from the diffuse reflected light from the reference.*

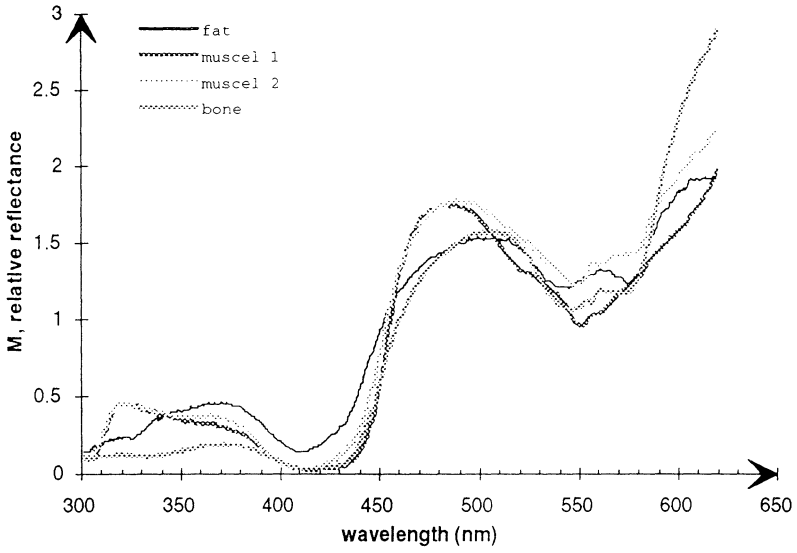


*Fig 19. The diffuse reflectance spectres from fat, muscle and bone tissue on a porkchop.*

Several measurements were made on the outside of the human body.

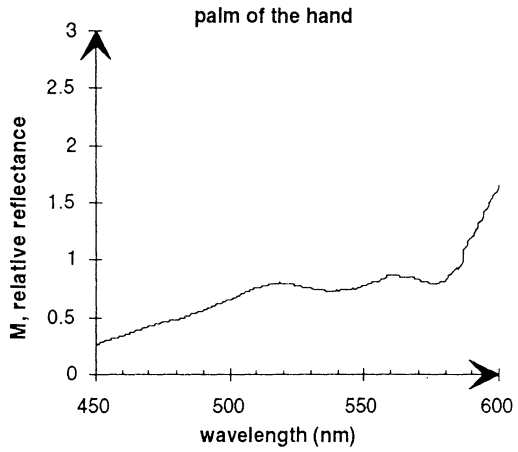


*Fig 20a.*

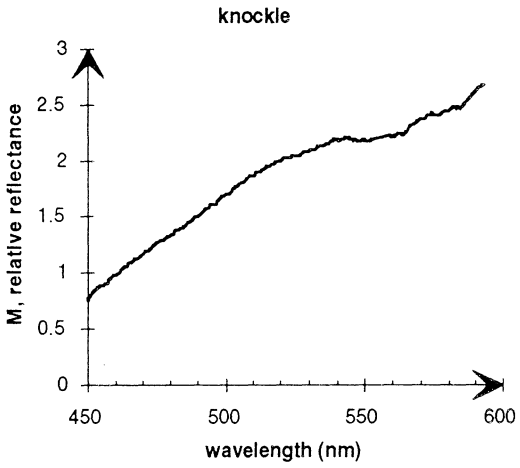


*Fig 20b.*

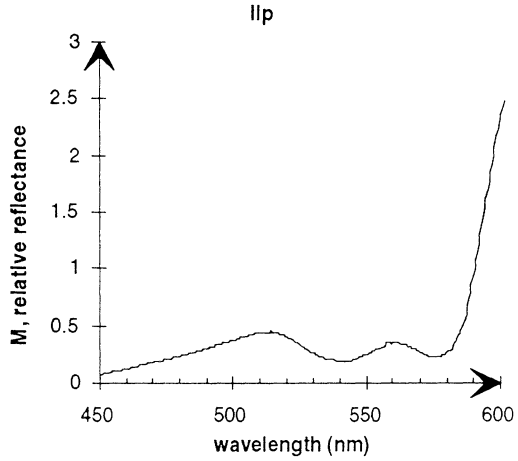


*Fig 20c.*

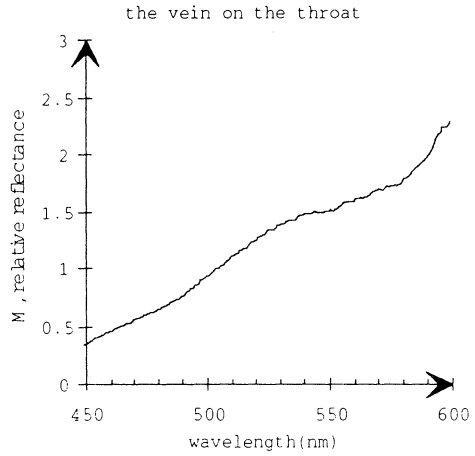


*Fig 20d.*

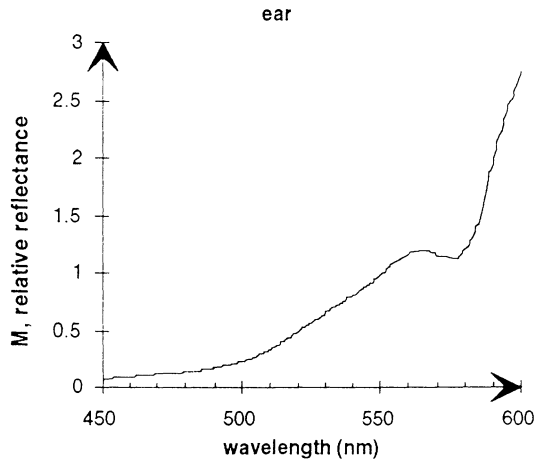


*Fig 20e.*

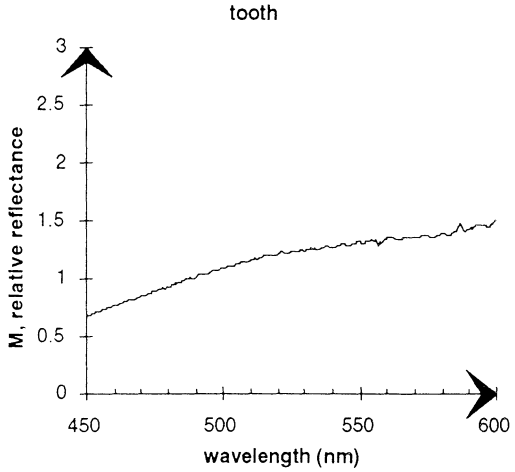


*Fig 20f.*

*Fig 20a-f. Diffuse reflectance spectra from different part on the human body.*

Finally recordings were collected from different human organs *in vitro*.

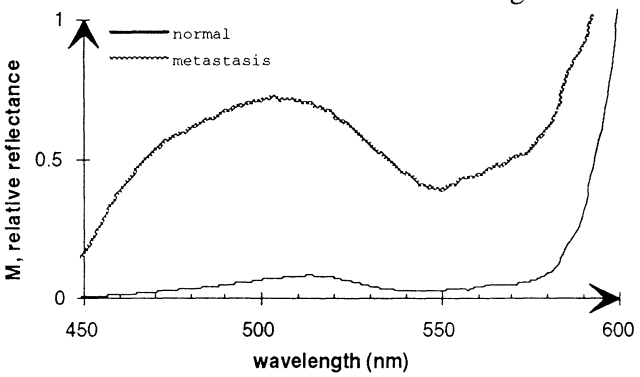


*Fig 21. Diffuse reflectance spectra from tissue sample from non-malignant liver and a liver metastasis*

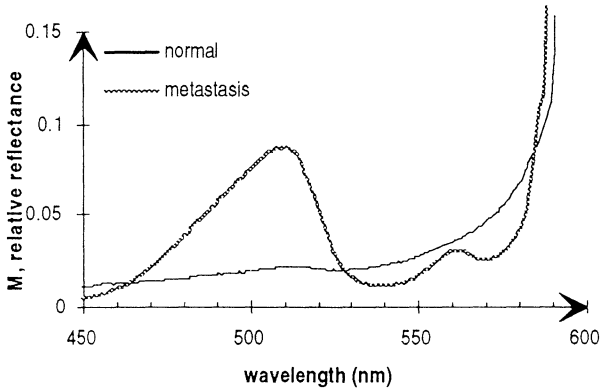


*Fig 22. Diffuse reflectance spectra from non-malignant lung and lung metastasis*

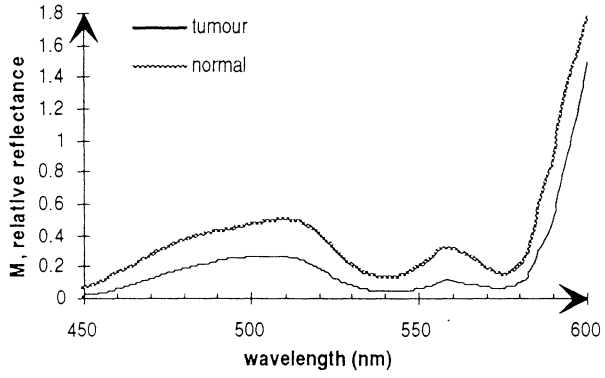


*Fig 23. Diffuse reflectance spectra from non-malignant testis and a testis tumour.*

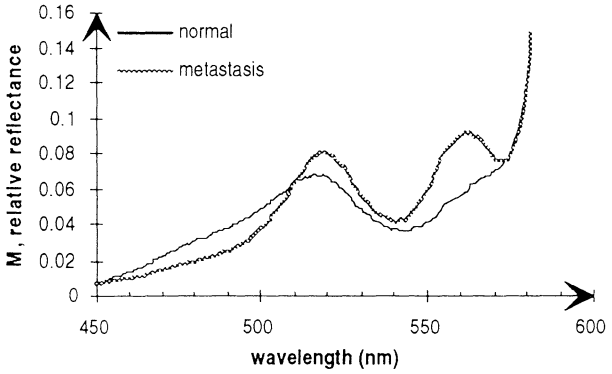


*Fig 24. Diffuse reflectance spectra from non malignant suprarenal gland and metastasis*

## 4.4 Measurements with the optical integrating sphere

Measurements were performed on the forearm with both the optical fiberprobe and with the optical integrating sphere. Plots are presented in Fig 25 to illustrate the difference between M, R and f.

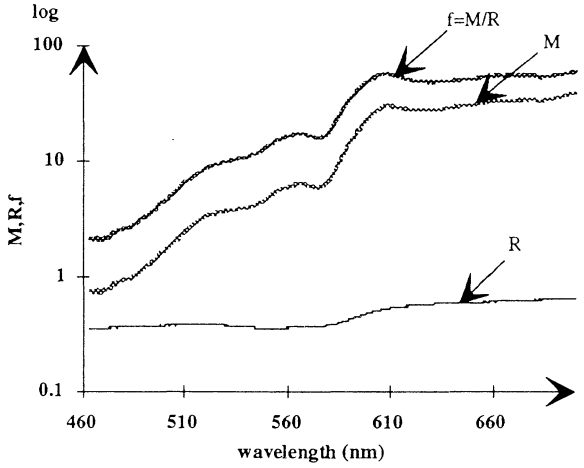


*Fig 25. A spectra of M, R and f from the forearm.*

## 4.5 Result from analyse of the skin recordings

Spectra from skin were analysed for melanin and blood content as described above. Spectra from a tanned and a untanned volunteer were recorded. Two spectra are presented in Fig 26.

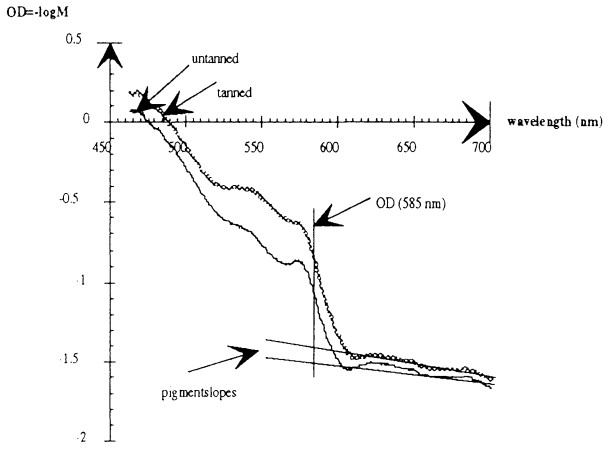


*Fig 26. OD spectra of a untanned and a tanned forearm*

Received data :

$\Delta OD_{585}$(tanned) =0.64 [OD]  pigment slope(tanned) = 869 [-OD/nm*$10^6$]

$\Delta OD_{585}$(untanned) =0.44 [OD]  pigment slope(untanned) = 714 [-OD/nm*$10^6$]

Analysed data:
% blood content (tanned) = 0.64 * 4.5[%/$\Delta OD_{585}$] = 2.9% equ. uniform blood vol.
% blood content (untanned) =0.44 * 4.5[%/$\Delta OD_{585}$] = 2.0% equ. uniform blood vol.

$f_{mel}$(tanned) = ( 869 - 600)(0.0126[%/slope]) = 3.4 % vol. fraction melanosomes
$f_{mel}$(untanned) = (714 - 600)(0.0126[%/slope]) = 1.4 % vol. fraction melanosomes

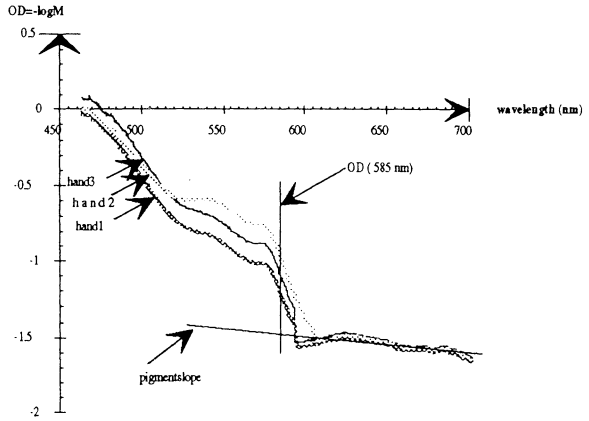

*Fig27. OD spectra from the dorsal side of the same hand*

Received data (all from the same hand):
$\Delta OD_{585}$ (hand1)=0.22 [OD]
$\Delta OD_{585}$(hand2) = 0.32 [OD]
$\Delta OD_{585}$(hand3) = 0.44 [OD]

pigment slope = 1000 [-OD/nm*$10^6$]

Analysed data:
% blood content (hand1) = 0.22 * 4.5[%/$\Delta OD_{585}$] = 1 % equ. uniform blood vol.
% blood content (hand2) = 0.32 * 4.5[%/$\Delta OD_{585}$] = 1.4 % equ. uniform blood vol.
% blood content (hand3) = 0.44 * 4.5[%/$\Delta OD_{585}$] = 2 % equ. uniform blood vol.

$f_{mel}$ = (1000 - 600)(0.0126[%/slope]) = 5.0 % vol. fraction melanosome

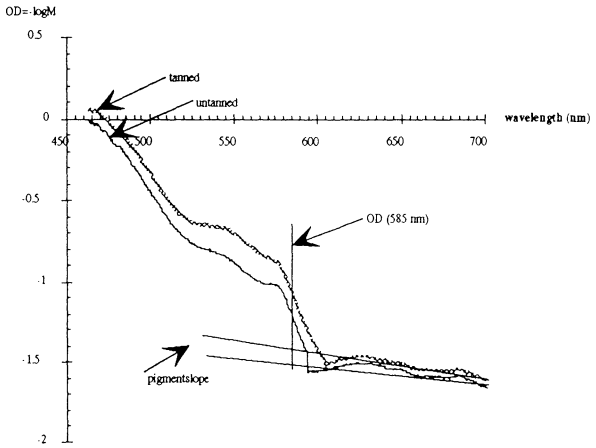

*Fig28. OD spectres of a tanned and an untannad above hand*

Received data :
$\Delta OD_{585}$(tanned) = 0.34 [OD]
$\Delta OD_{585}$(untanned) = 0.22 [OD]

pigment slope(tanned) = 1600 [-OD/nm*$10^6$]
pigment slope(untanned) = 1000 [-OD/nm*$10^6$]

Analysed data:

% blood content (tanned) = 0.34 * 4.5[%/$\Delta OD_{585}$] = 1.5% equ. uniform blood vol.

% blood content (untanned) = 0.22 * 4.5[%/$\Delta OD_{585}$] = 1.0 % equ. uniform blood vol.

$f_{mel}$(tanned) = ( 1600 - 600)(0.0126[%/slope]) = 8.8 % vol. fraction melanosomes

$f_{mel}$(untanned) = ( 1000 - 600)(0.0126[%/slope]) = 5.0 % vol. fraction melanosomes

# 5. Discussion and Conclusions

## 5.1 Discussion

The purpose with this work was to investigate an optical biopsy system for detection of cancer and other tissue pathologies. Several different organ areas and tissue types have been subject for the tests using two different setups, a monochromator-based and a OMA-based system.

Comparison between the monochromator and OMA-setups.
The first system, Monochromator-based system, was used and investigated, as the OMA-system was used in another project , but also because this setup was simpler and easier to handle than the OMA-system. There have been several problems to struggle with. It was difficult to get enough light and to get rid of the fluctuations of the Xenon lamp.

In order to get as good spectra as possible, one should work according to the following list:

- The equipment should be started at least 2 hours before the measurement, to let the lamp stabilise.
- The dwell time and time constant on the lock-in amplifier should be set to 5 second and to 1 second, respectively.
- The fibres should be put as close together as possible and as near the tissue sample as possible.
- The measurements should be performed in the dark, to avoid any influences from present background light.

With the OMA-system it was possible to measure further down in the ultraviolet region of the spectrum down to about 300 nm instead of 400 nm with the monochromator-based setup, figure 14-15 and figure 18-19. The OMA-system measures all wavelength at the same time while the Monochromator-based system measures one wavelength at a time. This makes that the OMA-system is more sensitive and less influenced by fluctuations in the lamp emission than the monochromator-based setup. The OMA-system was also used for most of the measurements in this study.

Comparison between the optical fibre probe and the optical integrating sphere.
The recorded spectra using the optical fibre probe depend, apart from the diffuse reflectance of the tissue also on the lamp emission spectrum, the detector response and on the fraction (f) of total reflectance collected by the fibre device. The collection fraction, f, depends on the optical properties of tissue, the fiberdiameter and the measurement geometry. Measurements of reflectance with the optical fibre probe has been performed, yielding the value M, from the skin area. The total diffuse reflectance, R, from the same skin area was also measured by an optical integrating sphere. The differences between M and R have been illustrated in Fig 25. M is related to R with a factor f* (f*=M/R). This factor is the ratio $f_{skin}/(R_{ref}f_{ref})$. The value of $f_{skin}$

could be calculated using equ.9 in chap.2.3 and the optical properties of bloodless dermis with 0.2% whole blood added[12]. $R_{ref}f_{ref}$ was deduced by $f_{skin}/f^*$. $R_{ref}$ is =0.992 and $f_{ref}$ is low because the light can spread broadly in the barium sulphate plug such that the fibre bundle collects only a small fraction of the reflected light. The actual measurements using both the optical integrating sphere and the optical fibre probe can be simulated using basic optical properties of tissues.
The dermal reflectance, epidermal melanin content and cutaneous blood content could be determined by the analysing of the recorded M spectra, as described by S.L Jacques[12].

A clear difference between the resulting M, R and $f^*$ spectra of skin was obtained. There are two minima in the curves and they are located to around 540 nm and 575 nm. These minima could be derived from the absorption peaks of haemoglobin, peaking of 542 and 577 nm. The M spectra have steeper slopes between 460-520 nm and above 580 nm as comparing to the R spectra. This is due to the dependence of the optical properties on the wavelength leading to clear dependence on the collected light fraction f, on the wavelength.

The same analysis as described in12 has been performed on some of the recorded spectra in this study. Figure 26 and 28 show spectra from measurements on a typical Swedish winterpale forearm and hand as well from a slightly tanned swedish forearm and hand, respectively. The analysis gave that the winterpale forearm contains a volume fraction of 1.4% of melansome in the epidermis and the sun-tanned forearm contains 3.4%. According to S.L.Jacques light skinned adults have a melansome volume fraction of 1.3-6.3%. Results obtained here fit quite well with this, the sun-tanned forearm contains more melanin than the pale forearm and Swedes are quite light skinned even though they are a bit sun-tanned.
The percentage blood content was in the range between 1% and 2% equ. uniform blood volume on the top of the hand and between 2% and 2.9% equ. uniform blood volume on the forearm. The levels depends somewhat on where on the hand or forearm measurements has taken place. There is no obvious difference between tanned and untanned skin.

Finally, measurement on human tissue has been performed *in vitro*. Only optical fibre measurements were made as this is how *in vivo* measurements can be performed. The recorded spectra have been analysed using the absorption spectra of haemoglobin. Normal liver tissue is absorbing strongly in the visible region of the spectrum as it contains much blood. At 515 nm normal liver tissue had a small maximum while the metastatic tumour has a stronger maximum otherwise both curves follows the Hb-curve. Both normal lung tissue and metastatic lung tumour shows a peak at 515 nm. Normal lung tissue spectrum has two dips at 535 nm and 570 nm while the tumour spectrum has dips at 560 nm and 585 nm.

## 5.2 Conclusions

If the Monochromator-based system is to be used, the equipment should be started at least 2 hours before the measurements. A mean value of at least three measurements at the same spot should be made before presenting the data. The recordings should be

performed in total darkness. The time constant and dwell time should be set to at least 3 seconds and 5 seconds, respectively. The Monochromator-based system could be used *in vitro* for pre-studie purposes. The OMA-system is better suited for continues measurements *in vitro* and *in vivo,* because this system is more sensitive to light, and as all wavelength is measured at the same time (any influences of fluctuation of light is avoided).

Comparisons between measurement with the optical integrating sphere and optical fibre probe have been made. Both types of spectra depends on the lamp emission spectrum and the detector response. However, the spectra recorded with the two-fibre probe also drastically depend of the collected fraction, f, as illustrated in Fig 25.

It is possible to distinguish differences between different kinds of tissues when studying the received diffuse reflection spectra. The most significant differences were found to be in the area of 450-550 nm. It is possible to relate reflection dips of the spectra as absorption peaks of haemoglobin. These are more or less accentuated in the spectra, depending on the blood content.
An analysing method described in chapter 3.4 has been used to extract some information of the percentage content of blood and the percentage volume fraction of melanosomes in tissue. The results are presented in chapter 4.5. In the recording presented here the forearm has higher blood content and less melanosomes than on the dorsal side of the hand.

The measurements on human tissue have been compared with each other and with the absorption spectra of haemoglobin. The spectra recorded from metastatic tumours showed, except for the testis tumour, more distinctive dips at 542-577 nm, than normal tissue.

## 5.3 Future

It would be desirable to get higher intensity on the incoming light. That would increase the intensity of the diffusely reflected light and make it possible to analyse more subtil differences between different types of tissue. One way to increase the incoming light would be to increase the number of fibres. The suggestion is to arrange seven fibres in a circle and make a fibrebundle. Three of these fibres could be used for incoming light and the rest could be used as light receiving fibres[3]. The fiber probe must satisfy many requirements to be useful in the clinical field, good optical characteristics, flexible, tough enough to go into the fibre endoscope and many more. The statistics in as well *in vitro* as *in vivo* measurements recorded in the laboratory must be performed before starting with clinical experiments. Before starting with clinical experiments a portable small optical spectrometer system should also be developed. A large number of clinical tests have already been performed by several scientists[3,4,16]. It seems that a diagnostic system based on diffused reflectance has large potential as a diagnostic tool and with a large variety of applications.

# 6. Acknowledgments

First of all I would like to thank my supervisors Annika Nilsson and Stefan Andersson-Engels, who have guided me throughout my work.

Then I would like to thank my fiancé Anders Bjerkén and my family for cheering me up when needed.

I would like to thank Claes af Klinteberg for helping me with computer problems.

I would also like to thank Unne Stenram at the Department of Pathology at Lunds University Hospital for the tissue sample I received and used in my experiments.

Finally I would like to thank everybody at the Department of Atomic Physics who have helped me with problems during this work, all included.

# 7. Reference List


1. B. C. Wilson and S. L. Jacques, Optical reflectance and transmittance of tissue: principles and applications, IEEE J. Quant. Electr. **16,** 155-167 (1992).

2. J. Boyer, J. R. Mourant, and I. J. Bigio, Theoretical and experimental investigations of elastic scattering spectroscopy as a potential diagnostic for tissue pathologies, in *Advances in Optical Imaging and Photon Migration,* R. R. Alfano , ed., OSA **21,** 265 -268 (Optical Society of America, Washington, DC, USA, 1994).

3. K. Ono, M. Kanda, J. Hiramoto, K. Yotsuya ,and N. Sato, Fiber optic reflectance spectrophotometry system for in vivo tissue diagnosis, Appl. Opt. **30,** 98-105 (1991).

4. I. J. Bigio, T. R. Loree, J. R. Mourant, T. Shimada, K. Story-Held, R. D. Glickman ,and R. Conn, "Optical diagnostics based on elastic scattering: recent clinical demonstration with the Los Alamos optical biopsy system," in *Optical Biopsy*, SPIE **2081,** 174 -184 (1993).

5. S. Svanberg, *Atomic and molecular spectroscopy* (Springer Verlag, Heidelberg, Germany, 1992).

6. E. M. Sevick, B. Chance, J. Leigh, S. Nioka and M. Maris, Quantitation of time- and frequency-resolved optical spectra for determination of tissue oxygenation, Analytical biochemistry **195,** 330-351 (1991).

7. W. F. Cheong, S. A. Prahl ,and A. J. Welch, A review of the optical properties of biological tissues, IEEE J. Quant. Electr. **26,** 2166-2185 (1990).

8. R. Berg, Laser-based cancer diagnostics and therapy - Tissue optics considerations, Dissertation thesis(Lund Institute of Technology, Lund, 1995).

9. A. M. K. Nilsson, R. Berg ,and S. Andersson-Engels, Measurements of the optical properties of tissue in conjunction with photodynamic therapy, Appl. Opt. **34,** 4609-4619 (1995) (LMLC-A1).

10. S. Svanberg, "Tissue diagnostics using lasers," in *Lasers in Medicine,* G. Pettit and R. W. Waynant, eds. (Wiley ,New York, USA ,1994) .

11. E. Hecht, *Optics* (Addison-Wesley Publishing Company, Reading, Massachusetts, USA, 1987).

12. S. L. Jacque, Reflectance spectroscopy with optical fiber devices, and transcutaneous bilirubinometers, Advanced Studies Institute, Erice, Sicily, Italy, NATO November 20, 1995.

13.P. Å. Öberg, "Laser-Doppler flowmetry," Crit. Rew. Biomed. Eng. **18,** 125-163 (1990).

14.I. J. Bigio, J. R. Mourant, J. Boyer ,and T. Johnson, Elastic scattering spectroscopy as a diagnostic for tissue pathologies, *CLEO '94*, (1994).

15.J. C. Fisher, Photons, physiatrics,and physicians: a practical guide to understanding laser light interaction with living tissue, part I, Journal of Clinical Laser Medicine & Surgery **10,** 419-426 (1996).

16.J. A. Zuclich, T. Shimada, T. R. Loree, I. J. Bigio, K. Strobl ,and S. Nie, Rapid noninvasive optical characterization of human lens, Lasers Life Sci. **6,** 39-53 (1994).